Chapter 7

Optical (UV-visible) Remote Sensing

Goal: Optical (UV/visible) theories for earth surface remote sensing.

7.1 The Optical (UV-Visible-Spectral) Range

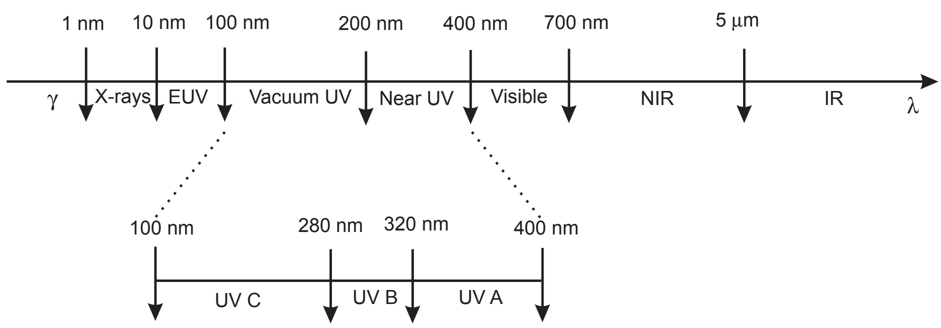

Figure 7.1: The optical (UV-visible-NIR) spectral range.

7.2 The Sun as a Light Source

The Solar spectrum can be approximated by a black body at temperature of 5780 K. It deviates from this black body at the top of the atmosphere because of absorption by molecules within the solar atmosphere which leads us to the Fraunhofer lines. In the atmosphere the solar radiation is attenuated in by scattering and absorption. Very strong absorbers are the molecules of O_3, O_2, H_2O and CO_2, but there are some atmospheric windows where absorption is small.

7.2.1 Multiple Light Paths when measuring with remote sensing the atmosphere

The first instruments to measure with remote-sensing technique the composition of trace gases within the atmosphere where ground-based. In principle, the ground-based instruments measure two possible light paths. Either solar occultation where the line of sight (LOS) of the instrument is oriented directly to the sun, or the LOS of the instrument is always oriented to zenith, i. e. zenith-sky measurements are obtained.

In practice, many light paths through the atmosphere contribute to the measured signal. Intensity measured at the surface consists of light scattered in the atmosphere in different altitudes. For each altitude, we have to consider the extinction on the way from the top of the atmosphere, the scattering probability and the extinction on the way to the surface. In the first approximation, the observed absorption is then the absorption along the individual light paths weighted with the respective intensity.

For solar occultation measurements the intensity of the direct sun light is so strong along the LOS that the signal from the other light paths can be neglected. So the retrieval from these measurements is much easier, but only under cloud-free conditions these measurements are possible.

Zenith sky measurements on the other hand are also possible under cloudy skies, but as described above because of the multiple light path complexity radiative transfer models are required in order to retrieve the information on the composition of the atmosphere.

With both techniques the absorber column density along the effective light path is retrieved, which is called the slant column density (SCD). In order to get the vertical column density (VCD) the air mass factor has to be used.

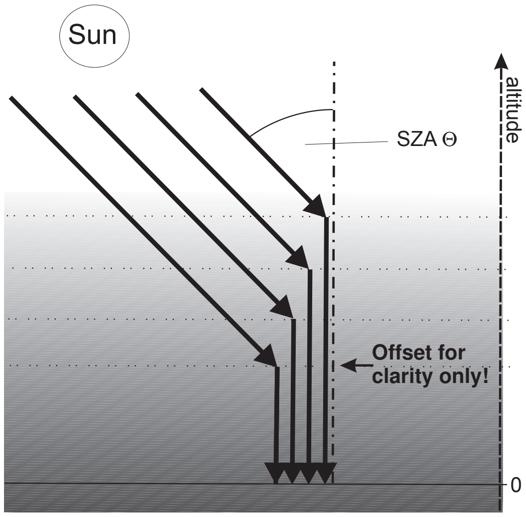

Figure 7.2: Multiple light paths through the atmosphere.

7.3 The Airmass Factor

The airmass factor (AMF) is the ratio of the measured SCD to the vertical VCD in the atmosphere. This means:

$$AMF = \frac{SC(\lambda\Theta, \dots)}{VC} \tag{7.1}$$

The AMF depends on variety of parameters such as:

- wavelength
- geometry
- vertical distribution of the species
- clouds
- aerosol loading
- surface albedo

The basic idea is that the sensitivity of the measurements depends on many parameters but if they are known, signal and column are proportional.

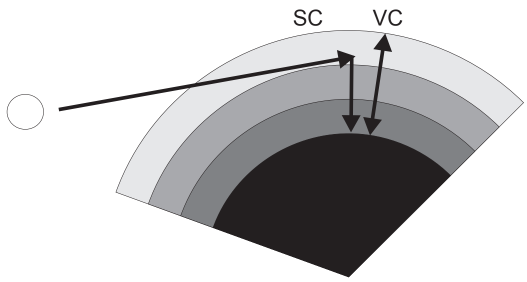

Figure 7.3: Ratio between slant and vertical column called the Air Mass Factor (AMF).

7.3.1 Dependence on Solar Zenith Angle (SZA)

For a **stratospheric absorber**, the AMF strongly increases with solar zenith angle (SZA) for ground-based, airborne and satellite measurements. A reason for this is the increasing light path in the upper atmosphere (geometry).

For an **absorber close to the surface**, the AMF is small, depends weakly on SZA, but at large SZA rapidly decreases. A reason for this is that the light path in the lowest atmosphere is short since it is after the scattering point for zenith observation.

From that it follows:
→ Stratospheric sensitivity is highest at large SZA (twilight)
→ Tropospheric sensitivity is largest at high sun (noon)
→ Diurnal variation of slant column carries information on vertical profile.

7.3.2 Dependence on Absorber Altitude

The AMF depends on the vertical profile of the absorber. The shape of the vertical dependence depends on the wavelength, viewing geometry and surface albedo. For the zenith viewing measurements, the sensitivity increases with the altitude (geometry). For satellite nadir observations, the sensitivity is low close to the surface over dark surfaces (photons don't reach the surface) but large over bright surfaces (multiple scattering).

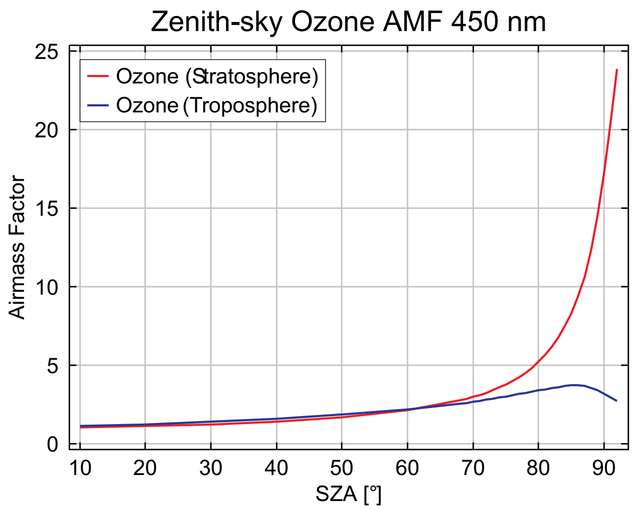

Figure 7.4: Airmass factor dependence on the zenith angle.

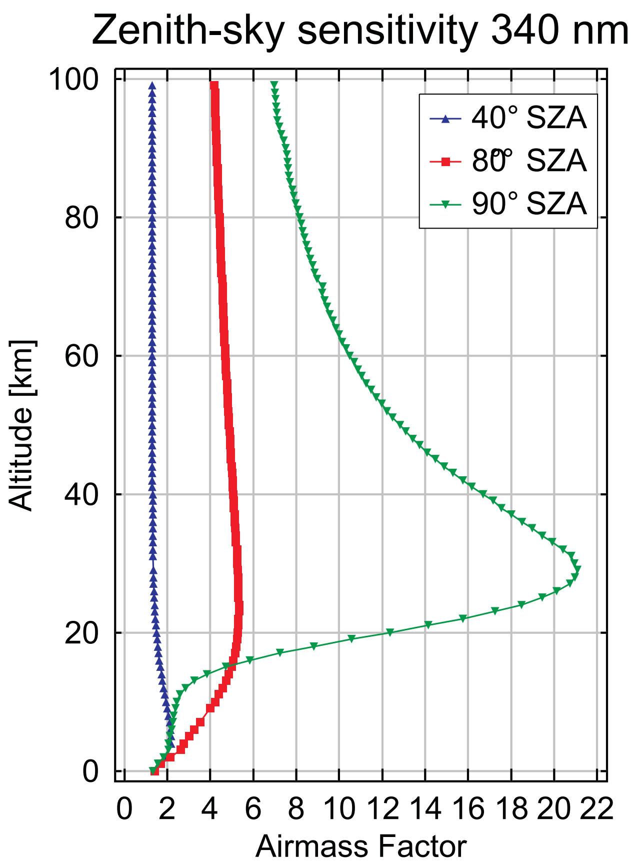

Figure 7.5: Dependence of the AMF on the absorber altitude.

From that it follows:
→ The vertical profile must be known for the calculation of AMF.

7.3.3 Dependence on Wavelength

The AMF depends on the wavelength as Rayleigh scattering is a strong function of wavelength and also the absorption varies with wavelength. At low sun, the AMF is smaller in the UV than in the visible as more light is scattered before traveling the long distance in the atmosphere. At high sun, the opposite is true as a result of multiple scattering.
UV measurements are more adequate for a large absorption. In case of the large absorptions, the nice separation of fit and radiative transfer is not valid anymore as AMF and absorption are correlated. Different wavelength "see" different parts of the atmosphere which can be used for the profile retrieval.

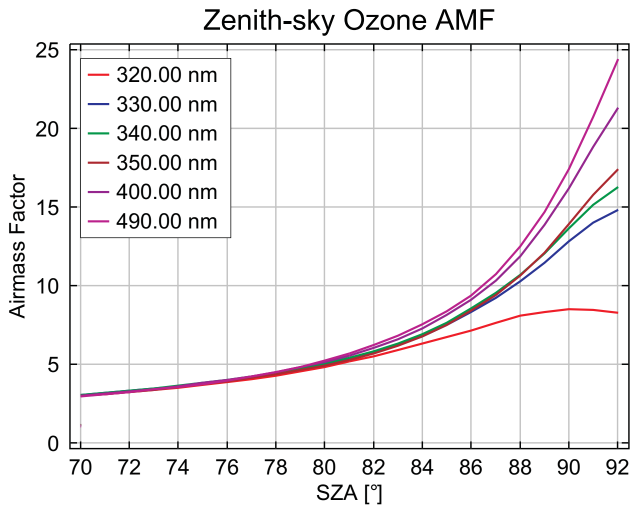

Figure 7.6: Dependence of the AMF on the wavelength.

7.4 Wavelength Pair Technique

The first remote sensing technique to measure ozone in the atmosphere is based on the measurement of the interval of two wavelengths within the UV region where at one wavelength ozone absorbs strongly, while at the other wavelength ozone absorption is weak. The Attenuatin of light at a particular wavelength is defined by the Lambert-Beer-Law where $I(\lambda)$ is the measured intensity after passing the molecule:

$$I(\lambda) = I_0(\lambda) \exp\left(-\sum \sigma(\lambda) n(x) dx\right) \tag{7.2}$$

From the ratio $I(\lambda)/I(\lambda')$ the Mie- and Rayleigh scattering cancelled out because it varies slowly with wavelength. For the Analysis the Lambert-beer's Law is used.

$$\frac{I(\lambda)}{I(\lambda')} = \frac{I_0(\lambda)}{I_0(\lambda')} \exp\left(-\sum \sigma(\lambda) n(x) dx + \sum \sigma(\lambda') n(x) dx\right) \tag{7.3}$$

Then the natural logarithm is taken:

$$\ln \frac{I(\lambda)}{I(\lambda')} = \ln \frac{I_0(\lambda)}{I_0(\lambda')} - (\sigma(\lambda) - \sigma(\lambda')) \sum (n(x) dx) \tag{7.4}$$

This measurement technique is used by the Dobson spectrometers (since 1927), the first remote sensing instruments to measure ozone with using the sun, the moon or scattered light as a light source. These instruments have high accuracy (2 percent relativ and +1-2 percent absolute) and good long term stability. A world wide network of these spectrometer (over 140 instruments are operating) consist and are the basis for validating satellite based ozone measurements.

7.5 DOAS Measurements

The DOAS method was invented as a remote sensing measurement technique of atmospheric trace gases in the atmosphere. Their measurement is based on absorption spectroscopy in the UV and visible wavelength range. Also to avoid problems with extinction by scattering or changes in the instrument throughput, so only signals that vary rapidly with wavelength are analyzed (thus the $differential$ in $DOAS$). These measurement are taken at moderate spectral resolution to identify and separate different species. While using the sun or the moon as light source, very long light paths can be realized in the atmosphere which leads to very high sensitivity. So even longer light paths are obtained at twilight when using scattered light. The scattered light observations can be taken at all weather conditions without significant loss in accuracy for stratospheric measurements. Also important is the use of simple, automated instruments for continuous operations.

7.5.1 The DOAS Equation

The intensity measured at the instruments is the extraterrestrial intensity weakened by absorption, Rayleigh and Mie scattering along the light path. The intensity is given by:

$$\begin{aligned} I(\lambda,\Theta) &= a(\lambda,\Theta) I_0(\lambda) * \\ &\exp\left(-\int\left(\sum_{j=1}^{J}\sigma_j(\lambda)\rho_j(s)+\sigma_{Mie}(s)\rho_{Mie}(s)+\sigma_{Ray}(\lambda)\rho_{Ray}(s)\right)ds\right) \end{aligned} \tag{7.5}$$

If the absorption cross-section does not vary along the line path s, we can simplify the equation by introducing the slant column SC, which is the total amount of the absorber per unit area integrated along the light path through the atmosphere. That means:

$$SC_j = \int \rho_j(s)ds \tag{7.6}$$

inserting into the DOAS equation, gives us:

$$\begin{aligned} \rightarrow I(\lambda,\Theta) &= a(\lambda,\Theta) I_0(\lambda) * \\ &\exp\left(-\sum_{j=1}^{J}\sigma_j(\lambda)SC_j - \sigma_{Mie}(\lambda)SC_{Mie} - \sigma_{Ray}(\lambda)SC_{Ray}\right) \end{aligned} \tag{7.7}$$

As Rayleigh and Mie scattering efficiency vary smoothly with wavelength, they can be approximated by low order polynomials. Also, the absorption cross-section can be separated into a high ("differential") and a low frequency part, the later of which can also be included in the polynomial.

$$\sigma_{Ray} \propto \lambda^{-4}; \qquad \sigma_{Mie} \propto \lambda^{-k}, \quad k = 0 \ldots 2; \qquad \sigma = \sigma_{low} + \sigma' \tag{7.8}$$

$$\begin{aligned} \to I(\lambda, \Theta) &= a(\lambda, \Theta) I_0(\lambda) \, * \\ &* \; \exp\left(-\sum_{j=1}^{J} \sigma_j(\lambda) SC_j - \sigma_{Mie}(\lambda) SC_{Mie} - \sigma_{Ray}(\lambda) SC_{Ray} \right) \end{aligned} \tag{7.9}$$

$$\to I(\lambda, \Theta) = a(\lambda, \Theta) I_0(\lambda) \exp\left(-\sum_{j=1}^{J} \sigma'_j(\lambda) SC_j + \sum_p b_p \lambda^p \right) \tag{7.10}$$

Finally, the logarithm is taken and the scattering efficiency included in the polynomial. The result is a linear equation between the optical depth, a polynomial and the slant columns of the absorbers. By solving it at many wavelengths (least squares approximation), the slant columns of several absorbers can be determined simultaneously. Thus gives us:

$$\left(\ln(\frac{I(\lambda, \Theta)}{I_0(\lambda)} \right) = -\sum_{j=1}^{J} \sigma'_j(\lambda) SC_j + \sum_p b^*_p \lambda^p \tag{7.11}$$

7.5.2 Examples for Satellite DOAS Data Analysis and DOAS Measurements

Nitrogene dioxide (NO_2) and NO are key species in tropospheric ozone formation. They also contribute to the acid rain generation. The sources are mainly anthropogenic (combustion of fossil fuels) but biomass burning, soil emission and lightning also contribute.

The GOME and SCIAMACHY are satellite borne DOAS instruments observing the atmosphere in nadir. This data can be analyzed for tropospheric NO_2 providing the first global maps of NO_X pollution.

7.6 Backscatter UV Ozone (Nadir) Measurements

Solar UV radiation reflected from the surface and backscattered by the atmosphere or clouds is absorbed by ozone in the Hartley-Huggins bands ($<$ 350 nm).

Note:

- most ozone lies in the stratosphere
- most of the backscattered UV-radiation comes from the troposphere
- little scattering occurs in the stratosphere
- radiation reaching the satellite passes through the ozone layer twice

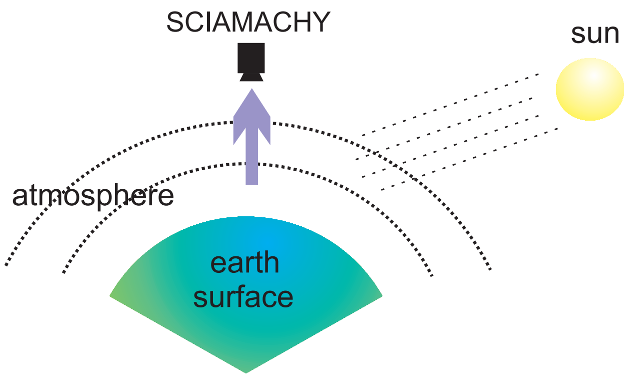

Figure 7.7: NADIR measurement scheme whereby the measured signal is reflected and scattered sunlight.

The backscatter UV-measurements allow retrieval of total O_3 columns and also vertical profiles, but with poor vertical resolution (7-10 km). They are taken in nadir geomtry. It measures O_3 slant column and uses a radiative transfer model to convert the slant column to a vertical column.
Examples:

- BUV (Backscatter Ultraviolet) instrument on Nimbus 4, 1970-1977
- SBUV (Solar Backscatter Ultraviolet) instrument on Nimbus 7, operated from 1978 to 1990
- SBUV/2 (Solar Backscatter Ultraviolet 2) instrument on the NOAA polar orbiter satellites (NOAA-11,14,15,16,17) measure since 1989 until today ozone profiles as well as columns
- TOMS (Total Ozone Mapping Spectrometer) first on NIMBUS 7, operated from 1978 to 1993. Then three subsequent versions: Meteor

3 (1991-1994), ADEOS (1997), Earth Probe (1996-2005) measure total ozone columns. Measurement technique is based on the discrete wavelength method.

- GOME (Global Ozone Monitoring Experiment) launched on ESA's ERS-2 satellite in 1995 employs a nadir-viewing BUV technique that measures radiances from 240 to 793 nm and also measures O_3 profiles, as well as columns of $NO_2, H_2O, SO_2, BrO, OCIO$, retirevals based on DOAS

- SCIAMACHY (Scanning Imaging Absorption spectroMeter for Atmospheric CHartographY): successor to GOME launched on Envisat in 2002 from 240 to 2400 nm measures even more species than GOME and also in limb and ocultation geometry, pixel size improved (30kmx60km)

- OMI (Ozone Monitoring Instrument): successor to GOME launched on AURA in 2004, measures only until 550 nm, but improved pixel size (18kmx13km), DOAS retrievals, bt for ozone also TOMS retrieval technique

7.7 Solar Occultation Measurements

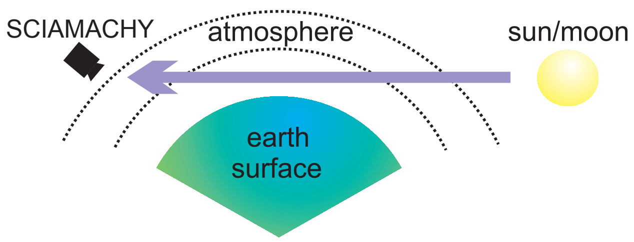

Figure 7.8: Occultation measurement scheme whereby mesured signal is directly transmitted solar radiation.

With $I_0(\lambda)$ as the spectrum at the highest tangent altitude with negligible atmospheric extinction and $I(\lambda, z_1)$ as spectrum at tangent altitude z_1 within the atmosphere. That will lead us to:

$$\exp\left(-\tau(\lambda, TH_i)\right) = \frac{I(\lambda, Th_i)}{I_0(\lambda)} = \exp\left(-\int_{LoS(TH_i)} \alpha_{ext.,\lambda}(x)dx\right) \quad (7.12)$$

LoS (line of sight):
With $\alpha_{ext.,\lambda}$ being the total extinction coefficient at position s along the line of sight. The extinction is usually due to Rayleigh-scattering, aerosol scattering and absorption by minor constituents:

$$\alpha_{ext.,\lambda}(x) = \alpha_\lambda^{Rayleigh}(x) + \alpha_\lambda^{aerosol}(x) + \alpha_\lambda^{gases}(x) \tag{7.13}$$

Due to the different spectral characteristics of the different absorbers and scatterers the optical depth due to, e.g. O_3 can be extracted:

$$\tau^{ozone}(\lambda, TH_i) = \int_{LoS} \underbrace{\sigma_{O_3}}_{\text{absorption cross section}}(x) \underbrace{n}_{O_3 \text{ number density}}(x)dx \tag{7.14}$$

If we assume that the cross-section does not depend on x, i.e., not on temperature and/or pressure, then

$$\tau^{ozone}(\lambda, TH_i) = \sigma_{O_3} \int_{LoS(TH_i)} n(x)dx = \sigma_{O_3} c(TH_i) \tag{7.15}$$

with the column density $c(z_i)$. The measurement provides a set of column densities integrated along the line of sight for different tangents altitudes z_i.
$\rightarrow$ Inversion to get vertical O_3 profile

Disadvantage of solar occultation measurements:
Measurements are only possible during orbital sunrises/sunsets. For typical Low Earth Orbits there are 14 - 15 orbital sunrises and sunsets per day.This leads to a poor geographical coverage.
Examples for solar occultation instruments:

- SAGE (Stratospheric Aerosol and Gas Experiment) Series provided continuous observations since 1981 to 2005. Latest instrument were SAGE 2 on ERBS (1984 to 2005) and SAGE 3 on Russian Meteor-3M spacecraft (2001 to 2005).

- POAM (Polar Ozone and Aerosol Measurements) series use UV-visible solar occultation to measure profile of ozone, H_2O, NO_2, aerosols measured until Spring 2006.

- GOMOS (Global Ozone Monitoring by Occultation of Stars) on Envisat performes UV-visible occultation using stars.

- SCIAMACHY (Scanning Imaging Absorption spectroMeter for Atmospheric CHartographY) on Envisat performs solar and lunar occultation measurements providing e.g., O_3, NO_2 and (nighttime) NO_3 profiles. It even operates since 2002.

- ACE-MAESTRO (Atmospheric Chemistry Experiment - Measurement of Aerosol Extinction in the Stratosphere and Troposphere Retrieved by Occultation) measures the 285-1030 nm region in two overlapping segments providing e.g., O_3, NO_2 and aerosol profiles. It operates since 2003.

7.8 UV/Visible Limb Measurements

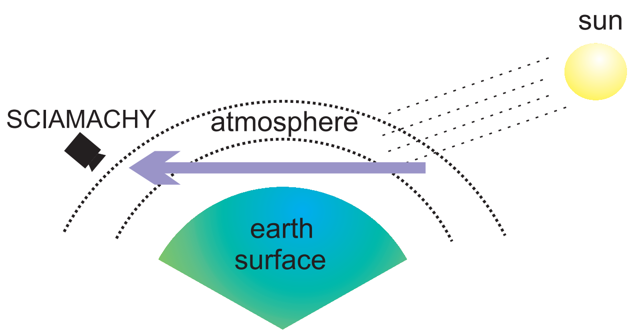

Figure 7.9: LIMB measurement scheme whereby the mesured signal is scattered solar radiation.

The Radiation is detected which is scattered into the field of view of the instrument along the line of sight and also transmitting from the scattering pint of the instrument. While the absorption signatures were picked up by the solar radiation along the way. Also the light path can be modified by atmospheric absorption. Vertical profiles of several trace constituents can be retrived from limb-scattered spectra employing a radiative transfer model (RTM) to simulate the measurements.
→ Retrival without forward model not possible

Examples for UV-visible Limb Sounders:

- SME (Solar Mesosphere Explorer) launched in 1981, carried the first ever limb scattered satellite instrument. MSX satellite was launched in 1996, carried a suite of UV-visible sensors (UVISI).
- SOLSE (Shuttle Ozone Limb Sounding Experiment) flown on the Space Shuttle flight in 1997. Provided good ozone profiles with high vertical resolution down to the tropopause.
- OSIRIS (Optical Spectrograph and Infrared Imaging System) launched in in 2001 on Odin satellite for retrival of vertical profiles of O_3, NO_2, OCIO and BrO.
- SCIAMACHY (Scanning Imaging Absorption SpectroMeter for Atmospheric CHartographY) launched on Envisat in 2002 for retrival of vertical profiles of O_3, NO_2, OCIO and BrO and aerosols.

7.9 Advantages and Disadvantages of Measurement Techniques

Technique	Advantages	Disadvantages
Nadir - Backscatter UV	• accurate • long time series • good horizontal resolution due to nadir viewing	• requires sunlight, so can't be used at night or over winter poles • poor vertical resolution below the the ozone peak (∼ 3km) due to the effects of multiple scattering and reduced sensitivity to the profile shape.
Occultation	• simple equipment • simple retrieval technique • good vertical resolution • self-calibrating	• can only be made at satellite while sunrise and sunset, which limits number and location of measurements • long horizontal path
Limb Scattering	• excellent spatial coverage • good vertical resolution • data can be taken nearly continously	• complex viewing geometry • poor horizontal resolution